Journal of
Biomedical Optics

SPIEDigitalLibrary.org/jbo

Vibrational spectroscopy: a tool being developed for the noninvasive monitoring of wound healing

Nicole J. Crane
Eric A. Elster

SPIE

Vibrational spectroscopy: a tool being developed for the noninvasive monitoring of wound healing

Nicole J. Crane[a] **and Eric A. Elster**[a,b,c]
[a]Naval Medical Research Center, Department of Regenerative Medicine, Silver Spring, Maryland 20910
[b]Walter Reed National Military Medical Center, Department of Surgery, Bethesda, Maryland 20892
[c]Uniformed Services University of the Health Sciences, Department of Surgery, Bethesda, Maryland 20892

Abstract. Wound care and management accounted for over 1.8 million hospital discharges in 2009. The complex nature of wound physiology involves hundreds of overlapping processes that we have only begun to understand over the past three decades. The management of wounds remains a significant challenge for inexperienced clinicians. The ensuing inflammatory response ultimately dictates the pace of wound healing and tissue regeneration. Consequently, the eventual timing of wound closure or definitive coverage is often subjective. Some wounds fail to close, or dehisce, despite the use and application of novel wound-specific treatment modalities. An understanding of the molecular environment of acute and chronic wounds throughout the wound-healing process can provide valuable insight into the mechanisms associated with the patient's outcome. Pathologic alterations of wounds are accompanied by fundamental changes in the molecular environment that can be analyzed by vibrational spectroscopy. Vibrational spectroscopy, specifically Raman and Fourier transform infrared spectroscopy, offers the capability to accurately detect and identify the various molecules that compose the extracellular matrix during wound healing in their native state. The identified changes might provide the objective markers of wound healing, which can then be integrated with clinical characteristics to guide the management of wounds. [DOI: 10.1117/1.JBO.17.1.010902]

Keywords: wound healing; acute wounds; chronic wounds; combat wounds; Raman spectroscopy; Fourier transform infrared spectroscopy.

Paper 11485V received Sep. 6, 2011; revised manuscript received Nov. 29, 2011; accepted for publication Nov. 30, 2011; published online Jan. 25, 2012.

1 Introduction

There is no healthcare specialty that is free from the morbidity and costs of wound development in a patient. In 2009, U.S. hospitals discharged over 1,300,000 patients with chronic wounds and more than 547,000 with traumatic wounds (classified as $>10\%$ body surface area burn or open wound).[1] U.S. healthcare costs related to wound treatment are well over $20 billion yearly, and the impact of wound healing on these expenditures is extensive.[2] In addition, if every surgical procedure is considered a case of an acute wound, the significance of wound healing is simply tremendous.

Although the wound-healing process of acute wounds such as surgical incisions is fairly well understood, the modified wound-healing process encountered in patients with chronic wounds and some traumatic acute wounds still requires elucidation. Normal healing of an acute wound is directed by a cascade of growth factors and cell signaling that allows the wounds to repair quickly. Chronic wounds and some traumatic acute wounds are much slower to heal and behave differently for several underlying reasons. There may be a pathologic process such as infection that prevents the wound from healing normally. Additionally, wound healing may be complicated by a prolonged inflammatory phase that inhibits normal levels of chemical mediators and cell recruitment. Finally, the patient's general condition contributes to the rate of wound healing; malnutrition and comorbidities such as diabetes are associated with impaired wound healing.[3]

Improved objective assessment of wounds would be conducive to better treatment of them, which might result in faster healing times, decreased infection rates, and decreased local and systemic complications of injury. For instance, if visits to the operating room were reduced by one instance per patient for 140 patients at one hospital, the cost savings would be over $2 million. The eventual timing of wound closure is often subjective, and there exists a need for an objective evaluation of the molecular environment of wounds throughout the wound-healing process. The use of vibrational spectroscopy and imaging for increased diagnostic accuracy and better wound treatment can produce improved clinical outcomes and decreased patient morbidity, resulting in an earlier return to an improved quality of life.

2 Wound Pathophysiology and the Process of Wound Healing

Several parameters are used to classify wounds: the layers of tissue involved, the origin and duration of the wound, and the type of wound closure used (i.e., surgical closure with sutures or formation of scar tissue). Origin and duration dictate whether a wound is classified as chronic or acute. Wounds resulting from trauma or surgery are acute wounds and generally proceed normally through the wound-healing process. An incision site in the abdomen, a third-degree burn, or a crushed limb

Address all correspondence to: Nicole J. Crane, Naval Medical Research Center, Department of Regenerative Medicine, Silver Spring, Maryland 20910. Tel: 301 319 7304; E-mail: Nicole.Crane@med.navy.mil

0091-3286/2012/$25.00 © 2012 SPIE

is termed an "acute wound." Wounds arising from chronic inflammation, repetitive insult, or vascular compromise that fail to heal normally or in a timely manner are called "chronic wounds." Pressure ulcers and diabetic foot ulcers are examples of chronic wounds. Acute wounds generally begin with a single, abrupt insult and progress through the healing process in an orderly manner. Conversely, chronic wounds are usually caused by a pathologic process such as infection or poor circulation.

In general, the wound-healing process proceeds through regeneration and/or repair. "Wound regeneration" is the renewal of the damaged tissue with healthy tissue that is the same, whereas "wound repair" is the replacement of the damaged tissue by scar tissue. Wounds that are confined to the superficial layers of skin heal by regeneration, but wounds that penetrate deep into the subcutaneous layers are not able to regenerate and heal by scar formation. The overall sequence of events that precedes injury is thought to be similar for chronic and acute wounds whereby chronic wounds simply stall at one or more stages during the wound-healing process.[4]

The first step in wound healing is hemostasis, the vascular response that triggers platelet activation and aggregation, clot formation, and vasoconstriction. The second step in wound healing is inflammation—capillaries vasodilate, and neutrophils and macrophages migrate to the wound bed to debride the wound and secrete growth factors to promote angiogenesis and connective tissue synthesis (tissue inhibitors of matrix metalloproteases, matrix metalloproteases, transforming growth factor-α and transforming growth factor-β, interleukin-1, interleukin-6, interleukin-8, epidermal growth factor, and keratinocyte growth factor). The third step in wound healing is proliferation, a multistep process involving epithelialization (early formation of the new wound bed from fibroblasts), neoangiogenesis (induction of new vasculature), and matrix and/or collagen deposition. The final step in wound healing is wound contraction and maturation and/or remodeling—the wound edges close, and a stronger, more orderly matrix forms scar tissue.[4]

Numerous factors that can affect the wound-healing process make an already complicated process even more difficult to accurately assess. These factors include age, stress, nutrition, tissue perfusion and oxygenation, infection, and other comorbidities, such as obesity, diabetes mellitus, immunosuppression, pulmonary disease, renal disease, and vascular disease. Unfortunately, in some cases, wound healing is complicated by dehiscence, in which "closed" wounds fall apart and reopen. The events leading up to wound dehiscence are not well understood but are suspected to result from an intensely exaggerated inflammatory response.[4] Currently, wounds are evaluated on the basis of parameters such as location of injury, adequacy of perfusion, gross appearance of the wound, wound tensile strength, and the patient's general condition. Although parameters such as the location of injury, the gross appearance of the wound, and the patient's general condition are fairly obvious and can be reasonably assessed, parameters such as the adequacy of perfusion and tensile strength are not readily quantifiable during surgery. It has previously been demonstrated that there is a greater incidence of associated vascular injury in slowly healing wounds than in normally healing wounds.[5] It is also well established that the tensile strength of the wound is dependent on collagen deposition.[6] There exists a need for technologies that can be used to noninvasively and objectively assess these challenging parameters.

3 Raman and Fourier Transform Infrared Spectroscopy

Raman and Fourier transform infrared (FTIR) spectroscopy are types of vibrational spectroscopy that measure the vibrational frequencies of molecules as the molecules are excited by incident photons. Every molecule has a unique fingerprint of vibrational frequencies, which makes Raman and FTIR spectroscopy highly specific techniques for molecular identification. Both techniques can be employed noninvasively, making them ideal for biomedical applications. Raman spectroscopy and FTIR spectroscopy are sometimes referred to as "sister" techniques and provide complementary information about molecules, but they differ in several fundamental ways.

Raman spectroscopy arises from the inelastic scattering of ultraviolet, visible, or near-infrared light when a photon interacts with a molecule. Raman scattering is an inherently weak process, and, as such, samples are typically illuminated by laser light. Light scattered by the sample is diffracted into individual wavelengths by a spectrograph and collected by a detector such as a CCD or CMOS sensor.[7] Raman systems can be coupled to a microscope and motorized stage for high-resolution imaging[8–14] or to a fiberoptic probe for bulk *in vivo* sampling.[15–20] Raman spectroscopy's independence from a specific sample thickness and lack of spectral interference from water make it an ideal technique for biomedical applications. One disadvantage of Raman spectroscopy in the biomedical arena, however, is its inherently weak signal, which can be overwhelmed by sample fluorescence. Often this is overcome by excitation in the near-infrared region of the spectrum where biological molecules tend not to fluoresce. There are other advanced configurations and applications of Raman spectroscopy, but they lie outside the scope of this review.[21–25].

FTIR spectroscopy consists of the absorbance of frequencies of light by a molecule that contains the same vibrational frequencies within its molecular bonds. A beam of infrared light is passed through or reflected by a sample. Some light is absorbed by the sample's vibrational frequencies, and the remaining light is transmitted to an interferometer and then collected by a detector, such as a mercury cadmium telluride photoconductive detector or an indium gallium arsenide photodiode detector.[26] As with Raman spectroscopic systems, FTIR systems can be coupled to a microscope[27–39] or a fiberoptic probe.[40] FTIR spectroscopy is sensitive to the presence of water, however, and *in vivo* sampling can be challenging. One disadvantage of FTIR spectroscopy is that it requires that light be able to pass through the sample and thus is confined to use with thin samples, such as tissue sections on optically transparent windows.

Both Raman spectroscopy and FTIR spectroscopy offer the capability to accurately detect and identify the various molecules that compose the extracellular matrix in their native state during wound healing. They are both imaging techniques in which the precise biochemical composition of biologic samples can be obtained by noninvasive and nondestructive means.[41–44] Both have been proven to be effective in studying tissues at the molecular level using diverse clinical and diagnostic applications, including the analysis of cellular structure and the determination of tumor grade and type.[9,42,45–48] Pathologic alterations of wounds are accompanied by fundamental changes in the molecular environment that can be analyzed by vibrational spectroscopy.[49,50] The identified changes might provide the objective markers of acute wound healing, which could then be integrated with clinical characteristics to guide the management of traumatic wounds. For instance, changes in collagen vibrational bands could be correlated with alterations in collagen deposition and reepithelialization of the wound bed.

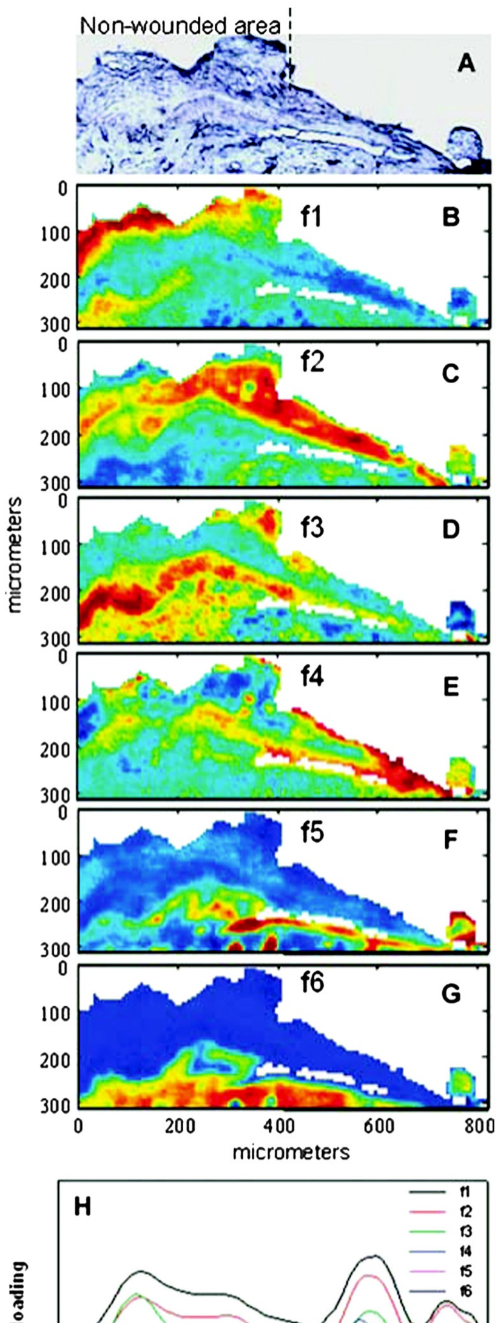

Fig. 1 Infrared characterization (factor analysis conducted over the 1185 to 1475/cm region) of wounded and nonwounded areas six days after wounding is shown. (a) Optical image of an unstained section with the edge of the wounded area marked by a vertical dashed line. (b—g) The score images are shown for various components of the tissue. (b) f1 is the stratum corneum and part of the viable epidermis. (c) f2 is the suprabasal epidermis. (d) f3 is the basal epidermal layer. (e) f4 is the outer leading edge of the migrating epithelial tongue. (f and g) f5 and f6 are the collagen-rich areas, respectively. (h) The factor loadings of f1 to f4 are characteristic of keratin-rich areas. The factor loadings of f5 and f6 are characteristic of collagen-rich areas. Reprinted with permission from John Wiley and Sons [J. Cell. Mol. Med. 12(5B), 2145–2154 (2008)].

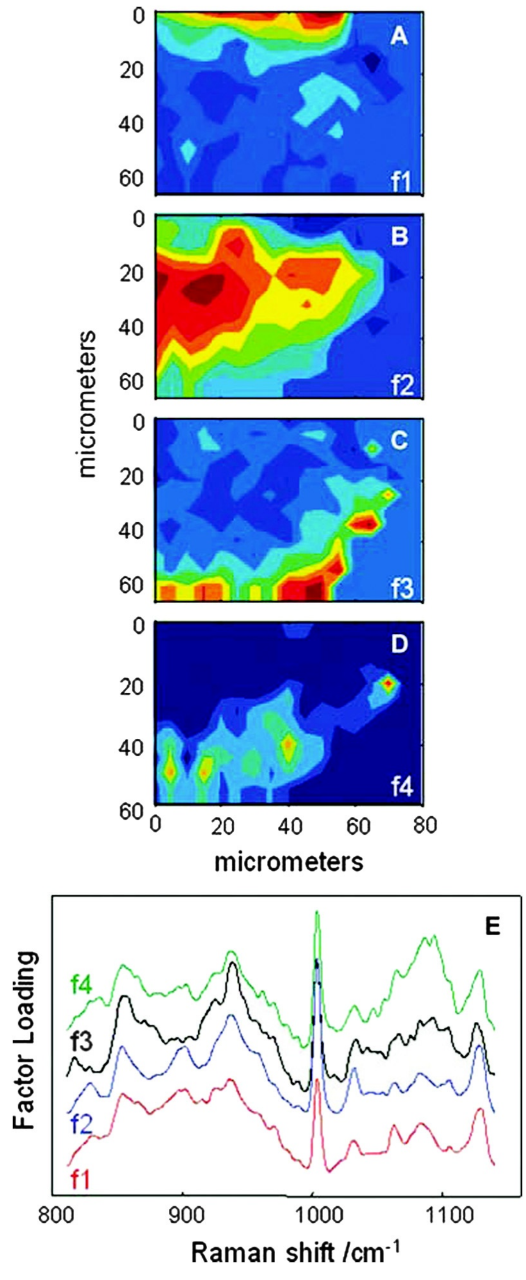

Fig. 2 Factor analysis of a confocal Raman dataset delineates skin regions near a wound edge 0.5 days after wounding. Data analysis was conducted over the 800 to 1140/cm region, yielding four factor loading images that map to anatomically distinct regions in the skin. (a) The spatial distribution of scores for f1 highlights the stratum corneum region of the skin, which is rich in keratin-filled corneocytes and lipids. (b) f2 shows high scores in the underlying epidermal region. (c) High scores for f3 reside near the dermal-epidermal boundary region. (d) The size, location, and spatial distribution of several smaller regions with high scores for f4 are identified as cell nuclei. (e) Factor loadings reveal several spectral features specific to the microanatomy of the epidermis in human skin. Reprinted with permission from John Wiley and Sons [J. Cell. Mol. Med. 12(5B), 2145–2154 (2008)].

4 Vibrational Spectroscopic Studies of Wound Healing

4.1 *Wounds*

The application of vibrational spectroscopy, such as Raman spectroscopy and FTIR spectroscopy, to study wound healing is a developing field of interest. Both *ex vivo* and *in vivo* models of wound healing have been explored in animals and humans, but all studies published to date have focused on acute wounds versus chronic wounds.

In all surgical cases, an acute wound is inflicted once a surgical incision is made. Thus, all surgical wounds are classified as acute wounds and are typically examples of the normal healing process. In early *ex vivo* studies by Wijelath and co-workers, FTIR attenuated total reflection (ATR) spectroscopy illustrated modified healing patterns in arterial grafts implanted into dogs. Standard histological analysis of the graft implants showed little or no activity in the first 10 days after implantation, but FTIR-ATR spectroscopy demonstrated changes within the fibrin layer of the graft that could be correlated to endothelialization of the wound.[51,52] Gough et al. utilized synchrotron FTIR spectroscopic mapping to monitor peridural scarring in rats following laminectomy.[53] Their results derived from untreated rats were compared to data from rats treated with L-2-oxothiazolidine-4-carboxylate (OTC). FTIR spectroscopic maps of laminectomized tissue sections indicated a decrease in lipid and phosphate bands, which are indicators of inflammatory cells. Immunohistochemistry confirmed these results and showed a diminished number of activated macrophages in OTC-treated rats. More recently, investigators successfully employed Raman spectroscopy to differentiate normal from injured tissue in rodent models of brain injury[54] and spinal cord injury.[55] In two rodent models of incisional wound healing, Raman spectra collected *in vivo* demonstrated increased protein configuration surrounding the wounds and increased cellularity[56] as well as conformational changes within the proteins themselves.[57]

To date, published applications of vibrational spectroscopy to study wound healing in humans have been performed on *ex vivo* biopsies of wounds. In 2008, Mendelsohn et al. utilized both FTIR and Raman spectroscopy to correlate spectroscopic changes with the reepithelialization of the wound bed of cutaneous incisional wounds.[49] Spectroscopic results were compared directly with immunohistochemical images of serial tissue sections and gene array analysis data. FTIR images collected four days after wounding precisely depicted the keratin-rich migrating epithelial tongue from the collagen-rich wound bed with focal data analysis of the 1185/cm to 1475/cm spectral region (Fig. 1). Similar spectral features are exhibited by factors 1 to 4 (f1 to f4), but the factors are spatially distinct within the sample itself. These represent keratin-rich areas confirmed by immunohistochemistry. Factors 5 and 6 are spectrally distinct from factors 1 to 4 and represent collagen-rich areas of the sample. Confocal Raman microspectroscopic images of tissue sections demonstrate the time dependence of elastin distribution in the wound up to six days after wounding (Fig. 2).[49] By day 2, the elastin distribution (f1) and the distribution of a collagen factor (f3) were significantly decreased, whereas the distribution of a second collagen factor (f2) decreased. Their study clearly demonstrates the utility of vibrational spectroscopy and imaging to monitor component-specific changes in skin in an acute wound-healing model.

Our group has used Raman spectroscopic mapping to monitor changes within the wound bed. Tissue biopsies were collected from Operation Iraqi Freedom and Operation Enduring Freedom combat-wounded soldiers at each surgical debridement during the wound-healing process.[58] Spectral maps revealed differences in the amide I/CH_2 scissoring band area ratios that correlated with wound outcome (Fig. 3), i.e., normal healing or impaired healing. Raman spectroscopic results were

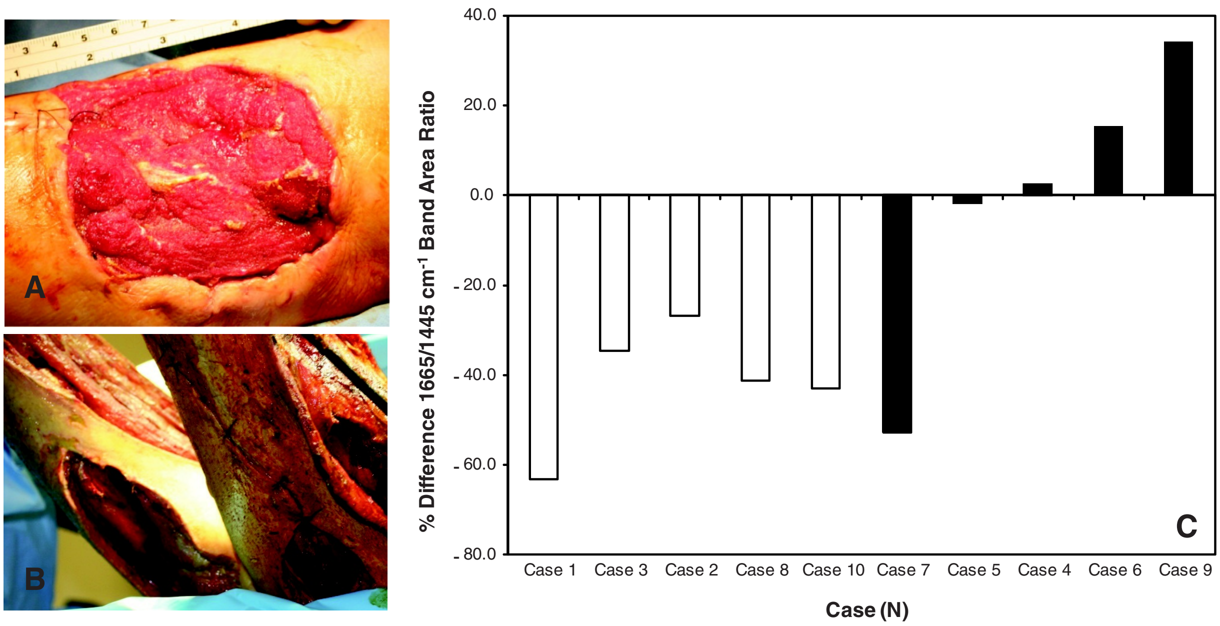

Fig. 3 Photographs are shown for a patient with a normal healing wound (a) and one whose wound healing was impaired (b). (c) This graph shows the percentage difference of the 1665-to-1445/cm band area ratios calculated from the first and last debridement 1665-to-1445/cm band area ratios for wounds classified as healing normally (black bars) and those wounds in which healing was classified as impaired (white bars).

corroborated with collagen gene expression profiles. In impaired healing wounds, a decrease in collagen-like bands was confirmed by decreased expression of the *COL1A1* and *COL3A1* genes (for type I and type III collagens, respectively).[58] In addition to monitoring the wound bed itself, FTIR and Raman spectroscopy were utilized to monitor complications of wound healing, such as infection, the formation of biofilm from subsequent infection, and heterotopic ossification (HO), to which acute and chronic wounds are susceptible.

4.2 *Infection*

For acute wounds such as surgical incisions, infection is the most prevalent postsurgical complication.[59] Chronic wounds provide a bed of growth for pathogens—they are warm, deep, and sometimes full of necrotic tissue. Chronic wounds are more often infected than acute wounds, but acute combat wounds present a subset of acute wounds with a high infection rate.[60] Identifying the pathogens responsible for wound bioburden is especially important because the prevalence of multi-drug-resistant bacteria is increasing, necessitating treatment with appropriate antimicrobial agents. Because of the specificity of Raman and FTIR spectroscopy, they can also be used to evaluate the bioburden of wounds. There have been numerous FTIR and Raman spectroscopic studies of microorganisms, many of which have been focused on rapid identification of the micro-organisms.[61–72] Differences in the Raman spectral profile of three bacterial species as well as three bacterial strains are evident in Fig. 4 (unpublished data). Both *Klebsiella pneumoniae* and *Acinetobacter baumannii* are Gram-positive bacteria, whereas methicillin-resistant *Staphylococcus aureus* is a Gram-negative bacterium. Differences in the Raman spectral profile, however, are due not strictly to peptidoglycan content but to other structural differences in the proteins as well. Inherent chemical differences in different bacterial species and strains, as demonstrated in Fig. 4, make possible the high specificity of Raman spectroscopy. When the Raman spectra of wound effluent collected from two patients colonized with different bacteria are compared (Fig. 4), the spectral profiles show differences in amino acid content and alterations in glycosidic linkages.

4.3 *Heterotopic Ossification*

Another complication of wound healing, "heterotopic ossification," is defined as the pathological formation of bone in soft tissue. HO formation has been observed following orthopedic surgery (total hip arthroplasty as well as acetabular and elbow fracture surgery), burn injury, traumatic brain injury, and spinal cord injury.[73] HO formation is not commonly observed in civilian traumatic wounds without the presence of head injury or spinal injury and develops in only 20% and 11% of these patients, respectively.[74] During the current military conflicts in Iraq and Afghanistan, HO has been a frequent and common clinical problem in soldiers with traumatic combat wounds. Currently, operative excision is the only treatment for mature, symptomatic HO. Identifying tissue that will develop into HO is not trivial, however, and can only be confirmed once mineralized tissue is evidenced on a radiograph. Tissue mineralization could easily be monitored with Raman spectroscopy.[12,75–88] Information could be gained that would reveal the quality of the bone being formed during HO. For example, is the bone "normal" but developing in soft tissue, or is the bone "pathological," developing by an different mineralization mechanism altogether.[80,89–94]

While Raman and FTIR spectroscopy have been used extensively to study the process of biomineralization,[84–95] they have not previously been used to provide insight into the pathological process of HO. We have collected Raman spectra of uninjured muscle, injured muscle, and "pre-HO" tissue (defined as palpably firm or "woody" tissue without roentgenographic evidence of HO) found within high-energy penetrating wounds (Fig. 5).[95] When we compared uninjured to injured muscle, we found an apparent decrease in the 1340 and 1320/cm vibrational bands in the injured muscle as well as an increase in the 1266/cm vibrational band. This suggests collagen-specific alterations within the tissue as a result of traumatic injury. In one case, a patient exhibited "pre-HO" muscle during a debridement procedure.

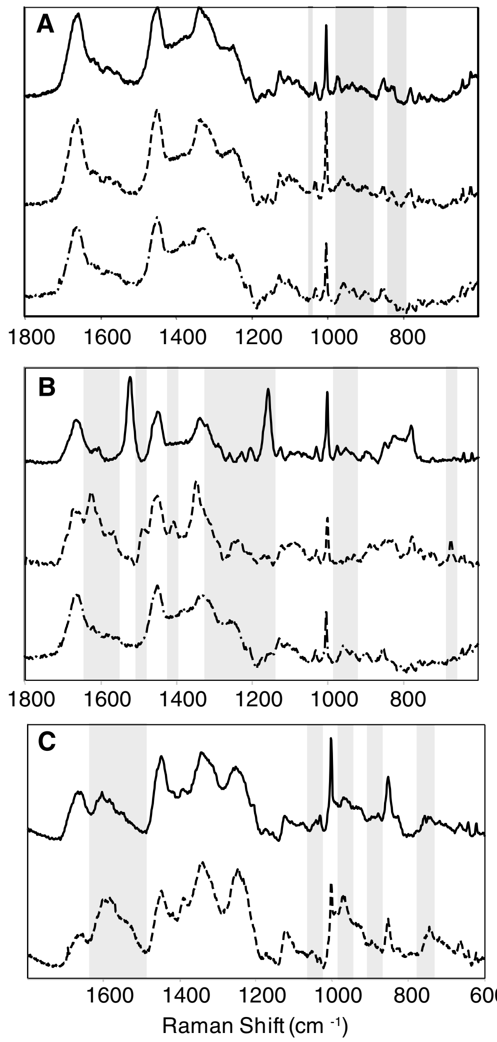

Fig. 4 Raman spectra of (a) methicillin-resistant *Staphylococcus aureus* (solid), *Klebsiella pneumoniae* (middle dashed line), and *Acinetobacter baumannii* (bottom dashed line). (b) Lines represent three different strains of *A. baumannii*. (c) Raman spectra obtained from wound effluent from a wound colonized with *Escherichia coli* (solid line) and from a wound colonized with *A. baumannii* (dashed line). Gray boxes highlight regions of the spectra where chemical differences are prevalent.

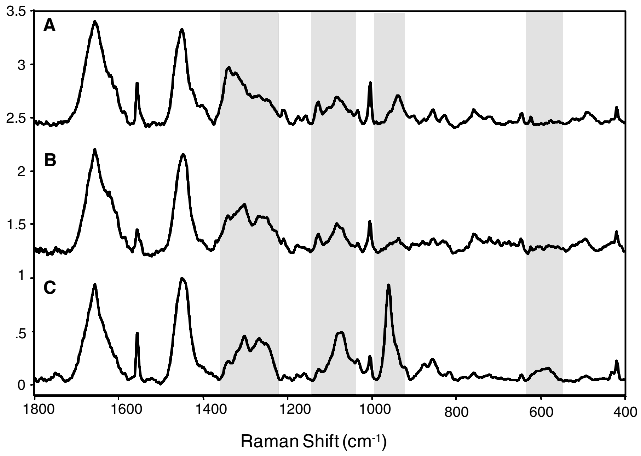

Fig. 5 Raman spectra of (a) uninjured muscle and/or control tissue, (b) combat-injured muscle, and (c) preheterotopic ossification combat-injured muscle. The gray boxes highlight spectral changes in the amide III envelope (1340 to 1240/cm) and the appearance of mineral vibrational bands at 1,070, 960, and 591/cm.

Upon Raman spectroscopic examination, it was clear that the tissue was indeed mineralized, even in "soft" tissue areas. Mineral vibrational bands at 1,070, 960, and 591/cm, typical of a carbonated apatite, were prominent in the spectrum. These vibrational bands are attributed to the phosphate and carbonate stretching modes of bone. Thus, Raman spectroscopy can potentially be utilized to identify areas of tissue affected by early HO as well as areas of tissue that may be predisposed to HO formation.

5 Conclusions

The potential of vibrational spectroscopy to provide detailed information, noninvasively, about molecular and even structural changes within the components of the wound bed itself enable a more thorough understanding of the wound-healing process. Vibrational spectroscopic modalities such as Raman and FTIR spectroscopy can provide an objective means of evaluation by monitoring key components of wound bed reepithelialization, such as keratin, elastin, and collagen; by identifying and quantifying bacterial load; and by detecting HO. These techniques have the potential to offer improved objective assessment of combat wounds, resulting in faster healing times, decreased infection rates, and decreased local and systemic complications of injury. This, in turn, will produce improved clinical outcomes, decreased patient morbidity, and reduced medical costs.

Acknowledgments

The views expressed in this paper are those of the authors and do not reflect the official policy of the Department of the Army, the Department of the Navy, the Department of Defense, or the U.S. government. We are military service members (or employees of the U.S. government). This work was prepared as part of our official duties. Title 17 U.S.C. § 105 states, "Copyright protection under this title is not available for any work of the United States Government." Title 17 U.S.C. § 101 defines a U.S. government work as a work prepared by a military service member or employee of the U.S. government as part of that person's official duties.

This effort was supported in part by the U.S. Navy Bureau of Medicine and Surgery under the Medical Development Program and Office of Naval Research work unit number 602115HP.3720.001.A1015. This study was approved by the National Naval Medical Center Institutional Review Board (NNMC IRB) in compliance with all federal regulations governing the protection of human subjects. The NNMC IRB-approved protocol number is NNMC.2005.0069/NMRC.2005.0012, and the protocol title is "The Use of Vacuum Assisted Wound Closure Device in the treatment of Extremity Wounds."

We certify that all individuals who qualify as authors have been listed; that each has participated in the conception and design of this work, the analysis of data (when applicable), the writing of the document, and the approval of the submission of this version; that the document represents valid work; that if we used information derived from another source, we obtained all necessary approvals to use it and made appropriate acknowledgments thereof in the document; and that each author takes public responsibility for it.

References

1. U.S. Department of Health & Human Services, Agency for Healthcare Research and Quality, *Healthcare Cost & Utilization Project (HCUP)*, August 22, 2011, http://www.ahrq.gov/data/hcup/, accessed December 30, 2011.
2. D. J. Samson, F. Lefevre, and N. Aronson, "*Wound-Healing Technologies: Low-Level Laser and Vacuum-Assisted Closure*", Evidence Report/Technology Assessment No. 111, prepared by the Blue Cross and Blue Shield Association Technology Evaluation Center Evidence-Based Practice Center under Contract No. 290-02-0026, AHRQ Publication No. 05-E005-2, December 2004, Rockville, MD, Agency for Healthcare Research and Quality, http://www.ahrq.gov/downloads/pub/evidence/pdf/woundtech/woundtech.pdf, accessed December 30, 2011.
3. R. A. Bryant and D. P. Nix, "Acute & Chronic Wounds: Current Management Concepts," 3rd ed., Mosby, St. Louis (2007).
4. R. A. Bryant and D. P. Nix, "Acute & Chronic Wounds: Current Management Concepts," 3rd ed., Mosby, St.Louis (2012).
5. J. S. Hawksworth et al., "Inflammatory biomarkers in combat wound healing," *Ann. Surg.* **250**6, 1002–1007 (2009).
6. F. C. Brunicardi et al., Eds., Schwartz's Manual of Surgery, 8th ed., McGraw-Hill, New York (2006).
7. I. R. Lewis and H. G. M. Edwards, Eds., "Handbook of Raman Spectroscopy: From the Research Laboratory to the Process Line", Marcel Dekker, New York (2001).
8. A. Kohler et al., "Multivariate image analysis of a set of FTIR microspectroscopy images of aged bovine muscle tissue combining image and design information," *Anal. Bioanal. Chem.* **389**4, 1143–1153 (2007).
9. T. Meyer et al., "Nonlinear microscopy, infrared, and Raman microspectroscopy for brain tumor analysis," *J. Biomed. Opt.* **16**2, 021113 (2011).
10. S. Keren et al., "Noninvasive molecular imaging of small living subjects using Raman spectroscopy," *Proc. Natl. Acad. Sci. U. S. A.* **105**15, 5844–5849 (2008).
11. M. Kazanci et al., "Bone osteonal tissues by Raman spectral mapping: orientation-composition," *J. Struct. Biol.* **156**3, 489–496 (2006).
12. M. D. Morris and W. F. Finney, "Recent developments in Raman and infrared spectroscopy and imaging of bone tissue," *Spectroscopy* **18**2, 155–159 (2004).
13. W. Gellermann et al., "Raman imaging of human macular pigments," *Opt. Lett.* **27**10, 833–835 (2002).
14. N. J. Kline and P. J. Treado, "Raman chemical imaging of breast tissue," *J. Raman Spectrosc.* **28**2–3, 119–124 (1997).
15. M. V. Schulmerich et al., "Subsurface and transcutaneous Raman spectroscopy and mapping using concentric illumination rings and collection with a circular fiber-optic array," *Appl. Spectrosc.* **61**7, 671–678 (2007).

16. Y. Hattori et al., "In vivo Raman study of the living rat esophagus and stomach using a micro-Raman probe under an endoscope," *Appl. Spectrosc.* **61**6, 579–584 (2007).
17. M. V. Schulmerich et al., "Transcutaneous Raman spectroscopy of bone tissue using a non-confocal fiber optic array probe," *Proc. SPIE* **6093**, 60930O (2006).
18. J. G. Wu et al., "Distinguishing malignant from normal oral tissues using FTIR fiber-optic techniques," *Biopolymers* **62**4, 185–192 (2001).
19. M. G. Shim et al., "Study of fiber-optic orobes for in vivo medical Raman spectroscopy," *Appl. Spectrosc.* **53**6, 619–627 (1999).
20. A. S. Haka et al., "In vivo margin assessment during partial mastectomy breast surgery using raman spectroscopy," *Cancer Res.* **66**6, 3317–3322 (2006).
21. J. Grun et al., "Identification of bacteria from two-dimensional resonant-Raman spectra," *Anal. Chem.* **79**14, 5489–5493 (2007).
22. C. A. Lieber et al., "In vivo nonmelanoma skin cancer diagnosis using Raman microspectroscopy," *Lasers Surg. Med.* **40**7, 461–467 (2008).
23. R. Manoharan et al., "Ultraviolet resonance Raman spectroscopy for detection of colon cancer," *Laser. Life Sci.* **6**4, 217–227 (1995).
24. K. R. Ward et al., "Oxygenation monitoring of tissue vasculature by resonance Raman spectroscopy," *Anal. Chem.* **79**4, 1514–1518 (2007).
25. P. S. Bernstein et al., "Resonance Raman measurement of macular carotenoids in the living human eye," *Arch. Biochem. Biophys.* **430**2, 163–169 (2004).
26. J. M. Chalmers and P. R. Griffiths, eds., Handbook of Vibrational Spectroscopy, vols. **5**, John Wiley & Sons, New York (2002).
27. C. Pezzei et al., "Characterization of normal and malignant prostate tissue by Fourier transform infrared microspectroscopy," *Mol. Biosyst.* **6**11, 2287–2295 (2010).
28. K. Wehbe et al., "FT-IR spectral imaging of blood vessels reveals protein secondary structure deviations induced by tumor growth," *Anal. Bioanal. Chem.* **392**1–2, 129–135 (2008).
29. E. Ly et al., "Combination of FTIR spectral imaging and chemometrics for tumour detection from paraffin-embedded biopsies," *Analyst* **133**2, 197–205 (2008).
30. C. Petibois et al., "Histological mapping of biochemical changes in solid tumors by FT-IR spectral imaging," *FEBS Lett.* **581**28, 5469–5474 (2007).
31. R. Bhargava, "Towards a practical Fourier transform infrared chemical imaging protocol for cancer histopathology," *Anal. Bioanal. Chem.* **389**4, 1155–1169 (2007).
32. C. H. Petter et al., "Development and application of Fourier-transform infrared chemical imaging of tumour in human tissue," *Curr. Med. Chem.* **16**3, 318–326 (2009).
33. B. Bird et al., "Infrared micro-spectral imaging: distinction of tissue types in axillary lymph node histology," *BMC Clin. Pathol.* **8**8, 8 (2008).
34. R. Zoehrer et al., "Bone quality determined by Fourier transform infrared imaging analysis in mild primary hyperparathyroidism," *J. Clin. Endocrinol. Metab.* **93**9, 3484–3489 (2008).
35. S. Gourion-Arsiquaud, P. A. West, and A. L. Boskey, "Fourier transform-infrared microspectroscopy and microscopic imaging," *Methods Mol. Biol.* **455**, 293–303 (2008).
36. X. Bi et al., "Fourier transform infrared imaging spectroscopy investigations in the pathogenesis and repair of cartilage," *Biochim. Biophys. Acta* **1758**7, 934–941 (2006).
37. E. David-Vaudey et al., "Fourier Transform Infrared Imaging of focal lesions in human osteoarthritic cartilage," *Eur. Cell Mater.* **10**, 51–60 (2005).
38. I. W. Levin and R. Bhargava, "Fourier transform infrared vibrational spectroscopic imaging: integrating microscopy and molecular recognition," *Annu. Rev. Phys. Chem.* **56**, 429–474 (2005).
39. D. C. Fernandez et al., "Infrared spectroscopic imaging for histopathologic recognition," *Nat. Biotechnol.* **23**4, 469–474 (2005).
40. V. K. Katukuri et al., "Detection of colonic inflammation with Fourier transform infrared spectroscopy using a flexible silver halide fiber," *Biomed. Opt. Express.* **1**3, 1014–1025 (2010).
41. C. Kendall et al., "Exploiting the diagnostic potential of biomolecular fingerprinting with vibrational spectroscopy," *Faraday Discuss.* **149**, 279–290 (2011).
42. C. Kendall et al., "Vibrational spectroscopy: a clinical tool for cancer diagnostics," *Analyst* **134**6, 1029–1045 (2009).
43. C. Krafft et al, "Raman and FTIR microscopic imaging of colon tissue: a comparative study," *J. Biophotonics* **1**2, 154–169 (2008).
44. C. Krafft et al., "Methodology for fiber-optic Raman mapping and FTIR imaging of metastases in mouse brains," *Anal. Bioanal. Chem.* **389**4, 1133–1142 (2007).
45. C. Krafft et al., "Disease recognition by infrared and Raman spectroscopy," *J. Biophotonics* **2**1–2, 13–28 (2009).
46. C. Murali Krishna et al., "An overview on applications of optical spectroscopy in cervical cancers," *J. Cancer Res. Ther.* **4**1, 26–36 (2008).
47. C. M. Krishna et al., "FTIR and Raman microspectroscopy of normal, benign, and malignant formalin-fixed ovarian tissues," *Anal. Bioanal. Chem.* **387**5, 1649–1656 (2007).
48. S. F. Weng et al., "FTIR fiber optics and FT-Raman spectroscopic studies for the diagnosis of cancer," *Am. Clin. Lab.* **19**7, 20 (2000).
49. K. L. Chan Andrew et al., "A coordinated approach to cutaneous wound healing: vibrational microscopy and molecular biology," *J. Cell. Mol. Med.* **12**5B, 2145–2154 (2008).
50. G. Chen et al., "Nonlinear spectral imaging of human hypertrophic scar based on two-photon excited fluorescence and second-harmonic generation," *Br. J. Dermatol.* **161**1, 48–55 (2009).
51. J. Murray-Wijelath, D. J. Lyman, and E. S. Wijelath, "Vascular graft healing. III. FTIR analysis of ePTFE graft samples from implanted bigrafts," *J. Biomed. Mater. Res. B Appl. Biomater.* **70**2, 223–232 (2004).
52. D. J. Lyman et al., "Vascular graft healing. II. FTIR analysis of polyester graft samples from implanted bi-grafts," *J. Biomed. Mater. Res.* **58**3, 221–237 (2001).
53. R. Wiens et al., "Synchrotron FTIR microspectroscopic analysis of the effects of anti-inflammatory therapeutics on wound healing in laminectomized rats," *Anal. Bioanal. Chem.* **387**5, 1679–1689 (2007).
54. L. L. Tay et al., "Detection of acute brain injury by Raman spectral signature," *Analyst* **136**8, 1620–1626 (2011).
55. T. Saxena et al., "Raman spectroscopic investigation of spinal cord injury in a rat model," *J. Biomed. Opt.* **16**2, 027003 (2011).
56. A. Makowski et al., "Laser preconditioning for wound healing: a Raman spectroscopy analysis," *Lasers Surg. Med.* **42**(Suppl. 22), 10–11 (2010).
57. A. Alimova et al., "In vivo molecular evaluation of guinea pig skin incisions healing after surgical suture and laser tissue welding using Raman spectroscopy," *J. Photochem. Photobiol. B* **96**3, 178–183 (2009).
58. N. J. Crane et al., "Monitoring the healing of combat wounds using Raman spectroscopic mapping," *Wound Repair Regen.* **18**4, 409–416 (2010).
59. A. J. Mangram et al., "Guideline for Prevention of Surgical Site Infection, 1999. Centers for Disease Control and Prevention (CDC) Hospital Infection Control Practices Advisory Committee," *Am. J. Infect. Control* **27**2, 96–134 (1999).
60. F. R. Sheppard et al., "The majority of US combat casualty soft-tissue wounds are not infected or colonized upon arrival or during treatment at a continental US military medical facility," *Am. J. Surg.* **200**4, 489–495 (2010).
61. P. C. Buijtels et al., "Rapid identification of mycobacteria by Raman spectroscopy," *J. Clin. Microbiol.* **46**3, 961–965 (2008).
62. M. F. Escoriza et al., "Raman spectroscopy and chemical imaging for quantification of filtered waterborne bacteria," *J. Microbiol. Methods* **66**1, 63–72 (2006).
63. K. Maquelin et al., "Identification of medically relevant microorganisms by vibrational spectroscopy," *J. Microbiol. Methods* **51**3, 255–271 (2002).
64. Q. Wu et al., "Intensities of E. coli nucleic acid Raman spectra excited selectively from whole cells with 251-nm light," *Anal. Chem.* **72**13, 2981–2986 (2000).
65. L. Zeiri et al., "Surface-enhanced Raman spectroscopy as a tool for probing specific biochemical components in bacteria," *Appl. Spectrosc.* **58**1, 33–40 (2004).
66. K. Maquelin et al., "Rapid epidemiological analysis of Acinetobacter strains by Raman spectroscopy," *J. Microbiol. Methods* **64**1, 126–131 (2006).
67. K. Maquelin et al., "Raman spectroscopic method for identification of clinically relevant microorganisms growing on solid culture medium," *Anal. Chem.* **72**1, 12–19 (2000).

68. K. S. Kalasinsky et al., "Raman chemical imaging spectroscopy reagentless detection and identification of pathogens: signature development and evaluation," *Anal. Chem.* **79**7, 2658–2673 (2007).
69. L. Zeiri et al., "Silver metal induced surface enhanced Raman of bacteria," *Colloids Surf A Physicochem. Eng. Asp* **208**, 357–362 (2002).
70. D. I. Ellis and R. Goodacre, "Metabolic fingerprinting in disease diagnosis: biomedical applications of infrared and Raman spectroscopy," *Analyst* **131**8, 875–885 (2006).
71. K. Maquelin et al., "Prospective study of the performance of vibrational spectroscopies for rapid identification of bacterial and fungal pathogens recovered from blood cultures," *J. Clin. Microbiol.* **41**1, 324–329 (2003).
72. C. L. Winder et al., "The rapid identification of Acinetobacter species using Fourier transform infrared spectroscopy," *J. Appl. Microbiol.* **96**2, 328–339 (2004).
73. F. S. Kaplan et al., "Heterotopic ossification," *Am. J. Acad. Orthop. Surg.* **12**2, 116–125 (2004).
74. D. E. Garland, "Clinical observations on fractures and heterotopic ossification in the spinal cord and traumatic brain injured populations," *Clin. Orthop. Relat. Res.* **233**, 86–101 (1988).
75. A. Carden and M. D. Morris, "Application of vibrational spectroscopy to the study of mineralized tissues," *J. Biomed. Opt.* **5**3, 259–268 (2000).
76. A. Carden et al., "Raman imaging of bone mineral and matrix: composition and function," *Proc. SPIE* **3608**, 132–138 (1999).
77. A. Carden et al., "Ultrastructural changes accompanying the mechanical deformation of bone tissue: a Raman imaging study," *Calcif. Tissue Int.* **72**2, 166–175 (2003).
78. C. J. de Grauw et al., "Investigation of bone and calcium phosphate coatings and crystallinity determination using Raman microspectroscopy," *Cells Mater* **6**1–3, 57–62 (1996).
79. M. D. Morris et al., "Bone microstructure deformation observed by Raman microscopy," *Proc. SPIE* **4254**, 81–89 (2001).
80. M. D. Morris et al., "Raman spectroscopy of early mineralization of normal and pathological calvaria," *Proc. SPIE* **4614**, 28–39 (2002).
81. M. D. Morris et al., "Raman microscopy of de novo woven bone tissue," *Proc. SPIE* **4254**, 90–96 (2001).
82. G. Penel et al., "Raman microspectrometry studies of brushite cement: in vivo evolution in a sheep model," *Bone* **25**(Suppl. 2), 81S–84S(1999).
83. G. Pezzotti and S. Sakakura, "Study of the toughening mechanisms in bone and biomimetic hydroxyapatite materials using Raman microprobe spectroscopy," *J. Biomed. Mater. Res.* **65A**2, 229–236 (2003).
84. J. A. Pezzuti et al., "Hyperspectral Raman imaging of bone growth and regrowth chemistry," *Proc. SPIE* **3261**, 270–276 (1998).
85. R. Smith and I. Rehman, "Fourier transform Raman spectroscopic studies of human bone," *J. Mater. Sci. Mater. Med.* **5**, 775–778 (1995).
86. C. P. Tarnowski, M. A. Ignelzi, Jr., and M. D. Morris, "Mineralization of developing mouse calvaria as revealed by Raman microspectroscopy," *J. Bone Miner. Res.* **17**6, 1118–1126 (2002).
87. J. Timlin et al., "Raman spectroscopic imaging markers for fatigue-related microdamage in bovine bone," *Anal. Chem.* **72**10, 2229–2236 (2000).
88. J. A. Timlin et al., "Spatial distribution of phosphate species in mature and newly generated mammalian bone by hyperspectral Raman imaging," *J. Biomed. Opt.* **4**1, 28–34 (1999).
89. N. J. Crane et al., "Raman spectroscopic evidence for octacalcium phosphate and other transient mineral species deposited during intramembraneous mineralization," *Bone* **39**3, 434–442 (2006).
90. J. J. Freeman et al., "Raman spectroscopic detection of changes in bioapatite in mouse femora as a function of age and in vitro fluoride treatment," *Calcif. Tissue Int.* **68**3, 156–162 (2001).
91. M. D. Morris et al., "Effects of applied load on bone tissue as observed by Raman spectroscopy," *Proc. SPIE* **4614**, 47–54 (2002).
92. J. D. Pasteris et al., "Lack of OH in nanocrystalline apatite as a function of degree of atomic order: implications for bone and biomaterials," *Biomaterials* **25**2, 229–238 (2004).
93. G. Penel et al., "MicroRaman spectral study of the PO_4 and CO_3 vibrational modes in synthetic and biological apatites," *Calcif. Tissue Int.* **63**6, 475–481 (1998).
94. P. Taddei et al., "Vibrational spectroscopic characterization of new calcium phosphate bioactive coatings," *Biospectroscopy* **57**3, 140–148 (2000).
95. B. K. Potter et al., "Heterotopic ossification following combat-related trauma," *J. Bone Joint Surg. Am.* **92**(Suppl. 2), 74–89(2010).